ELSEVIER

Composites Science and Technology 54 (1995) 223–232
Elsevier Science Limited
Printed in Northern Ireland

0266-3538(95)00054-2

MODELING OF DELAMINATION BUCKLING IN COMPOSITE CYLINDRICAL SHELLS WITH A NEW HIGHER-ORDER THEORY

Aditi Chattopadhyay & Haozhong Gu

Department of Mechanical and Aerospace Engineering, Arizona State University, Tempe, Arizona 85287-6106, USA

(Received 7 December 1994; revised version received 13 March 1995; accepted 3 April 1995)

Abstract

A higher-order shear deformation theory has been employed for evaluating accurately the transverse shear effects in delamination buckling of cylindrical shells under axial compression. The governing differential equations of the present theory are obtained by applying the principle of the stationary value of the total potential. The Rayleigh–Ritz method is used to solve the equations by assuming a double Fourier expansion of the displacements with trigonometric coordinate functions. Numerical results for linear delamination buckling of axially compressed cylindrical shells with clamped ends are presented to validate the theory. Comparisons are made with the classical laminate theory and first-order theory results.

Keywords: buckling, composites, delamination, higher-order theory, cylindrical shells

INTRODUCTION

The problem of delamination buckling of composite laminates has generated significant research interest and has been the subject of several theoretical investigations.[1–3] However, questions still remain regarding a complete understanding and details of the phenomena involved. The problem of delamination buckling of cylindrical shells has not received adequate attention; very few investigations have been reported in this area. Two separate studies were reported,[4,5] for solving the problem of buckling of layered cylindrical shells. The effect of longitudinal delamination, assumed to extend over the entire length of the shell, in a laminar cylindrical shell subject to external pressure has been examined.[6] A more advanced model was presented[7] for the study of delamination buckling of axially loaded cylindrical shells. The delamination instability of long cylindrical panels[8] and thin complete cylindrical shells with finite length[9] subjected to external pressure has been studied. Further investigation was performed[10] for the delamination effect on the response of cylindrical composite shells subjected to external loadings, in which the prediction of postbuckling behavior was provided. Moreover, the thin film model approximation for the problem of delamination buckling in external pressure-loaded laminated cylindrical shells has been introduced,[11] in which the unbuckled portion of the shell was considered 'infinitely thick' with respect to the delamination layer, and the first approximation scheme was used to derive the close-form expressions of the critical pressure. With few exceptions, the analyses of multilayered cylindrical shells have been conducted only by using the classical laminate theory based on the Kirchhoff hypothesis.

A number of recent investigations have pointed out that the classical laminate theory is adequate for isotropic shells only when the thickness-to-radius ratio is very small.[3,12–14] Also, when fiber-reinforced composites are considered, the transverse shear strains must be taken into account since the ratio between the layer extentional modulus along the fiber direction and the shear modulus is usually very large.[14] Many efforts have been made in developing various two-dimensional shear deformable laminate theories,[15–25] three-dimensional layer-wise techniques,[14] three-dimensional finite element models[26] and even exact elasticity solutions[12,13] to address the buckling problem of composite cylindrical shells without delamination. However, in the presence of delamination, the regular two-dimensional theories are no longer valid since in such a problem the transverse shear stresses must vanish not only at the surfaces but also at the delaminated interfaces. Therefore, a higher-order shear deformation theory (excluding the first-order theory) for addressing delamination modeling in composites cannot be a simple extension of the regular theory. Recently, a new higher-order shear deformation theory has been presented[27] to address delamination buckling of composite plates. By

modifying the displacement field of regular higher-order theory,[28] an appropriate kinematic field, which can describe separation and slipping between the delaminated layer and the sub-laminate, was proposed. Some higher-order shear correction terms were identified to ensure that the refined displacement field satisfies the transverse shear stress-free boundary conditions at both plate surfaces and debonding interfaces. The results obtained using the new theory showed excellent agreement with available experimental data for composite plates. It was shown that the new theory provides an effective solution for accurate analysis of composite laminates with delaminations.

Composite laminated cylindrical shells are often used as a primary load-carrying structure in aerospace vehicles. Therefore, to ensure structural integrity and life of the vehicle, it is now of interest to develop accurate analysis procedures for modeling composite shells with pre-existing delaminations. A generalized consistent theory is considered to provide a better insight into the deformation and failure mechanism of these structures.

In this paper, the new higher-order shear deformable theory, which was developed previously[27] is extended to model delamination buckling of cylindrical shells of perfect geometry and under uniform axial compression. The governing differential equations of the present theory are obtained by applying the principle of the stationary value of the total potential. The displacements are expressed using a double trigonometric expansion and the Rayleigh–Ritz method is employed to obtain a set of algebraic equations. Numerical results are presented and are compared with existing solutions.

MATHEMATICAL FORMULATION

For laminated circular cylindrical shells, the new higher-order theory is used to describe accurately the displacement components, as follows:

$$u_\alpha = \sum_{j=0}^{N} z^j\{U_{\alpha j}^{(0)} + [1 - H(z^*)]U_{\alpha j}^{(1)} + H(z^*)U_{\alpha j}^{(2)}\} \quad (1)$$

$$u_3 = W^{(0)} + [1 - H(z^*)]W^{(1)} + H(z^*)W^{(2)};\ \alpha = 1, 2$$

where u_i $(i = 1, 2, 3)$ are the displacement components, z^* is the distance measured from the shell mid-surface to the delamination interface, $(U_{\alpha 0}^{(0)}, W^{(0)})$ are the displacements at a point x_α $(\alpha = 1, 2)$ on the mid-surface, $U_{\alpha j}^{(0)}$ $(j = 1, 2, \ldots N)$ are the jth order transverse shear correction terms and $H(z^*)$ is the Heaviside step function which is described as follows:

$$H(z^*) = H(z - z^*) = \begin{cases} 1 & z \geq z^* \\ 0 & z < z^* \end{cases} \quad (2)$$

The jumps in displacement between the sublaminate layer and the buckling layer are given by $U_{\alpha j}^{(1)}$, $W^{(1)}$ and $U_{\alpha j}^{(2)}$, $W^{(2)}$ $(\alpha = 1, 2;\ j = 0, 1, \ldots N)$, respectively. Note that the terms related to the delamination, $U_{\alpha j}^{(k)}$ and $W^{(k)}$ $(k = 1, 2)$, only exist in the delamination region Ω_d. The use of the step function, $H(z^*)$, allows the kinematic description for separation and slipping due to the independence of the displacements, shown in eqn (1), on adjacent layers at the delamination interface.

In the buckling analysis, the following linear strain-displacement relationships are used.

$$\begin{aligned} \varepsilon_1 &= \varepsilon_{11} = u_{1,x} \\ \varepsilon_2 &= \varepsilon_{22} = u_{2,y} + \frac{u_3}{R} \\ \varepsilon_4 &= 2\varepsilon_{23} = u_{2,z} + u_{3,y} - \frac{u_2}{R} \\ \varepsilon_5 &= 2\varepsilon_{13} = u_{1,z} + u_{3,x} \\ \varepsilon_6 &= 2\varepsilon_{12} = u_{1,x} + u_{2,y} \end{aligned} \quad (3)$$

where ε_i are strain components and R is the radius of curvature of the cylindrical shell. The layer constitutive equation can be written as follows:

$$\sigma_i = Q_{ij}\varepsilon_j, \quad i, j = 1, 2, \ldots, 6 \quad (4)$$

where σ_i are the stress components and Q_{ij} are the lamina stiffness components of the shell.

It must be noted that the expression for displacement, as stated in eqn (1), does not satisfy the transverse shear stress-free boundary conditions. These stress-free boundary conditions, in delamination problems, require that the transverse shear stresses, σ_4 and σ_5, vanish on the shell inner and outer surfaces and on the debonding surfaces in the delamination region. That is:

$$\begin{aligned} &\sigma_4(x, y, \pm h/2) = 0, \\ &\sigma_5(x, y \pm h/2) = 0, \quad (x, y) \in \Omega \\ &\sigma_4^{\pm}(x, y, z^*) = 0, \\ &\sigma_5^{\pm}(x, y, z^*) = 0, \quad (x, y) \in \Omega_d \end{aligned} \quad (5)$$

in which h is the shell thickness and the superscripts '+' and '−' refer to the quantities related to the buckling layer and the sublaminate layer, respectively. For orthotropic layers of shells, the conditions are equivalent to the requirement that the corresponding strains be zero on these surfaces. Therefore:

$$\begin{aligned} &\varepsilon_4(x, y, \pm h/2) = 0, \\ &\varepsilon_5(x, y, \pm h/2) = 0, \quad (x, y) \in \Omega \\ &\varepsilon_4^{\pm}(x, y, z^*) = 0, \\ &\varepsilon_5^{\pm}(x, y, z^*) = 0, \quad (x, y) \in \Omega_d \end{aligned} \quad (6)$$

Applying these stress-free boundary conditions to eqn

(3) and using the displacement expression, eqn (1), a total of 12 equations should be solved to obtain the unique form of refined displacement field. These equations are as follows:

$$\sum_{j=1}^{N} jz^{j-1}U_{1j}^{(0)}(x, y, \pm h) + W_{,x}^{(0)}(x, y, \pm h) = 0 \quad (x, y) \in \Omega$$

$$\sum_{j=1}^{N} jz^{j-1}U_{2j}^{(0)}(x, y, \pm h) + W_{,y}^{(0)}(x, y, \pm h) - \frac{1}{R}\sum_{j=0}^{N} z^j U_{2j}^{(0)}(x, y, \pm h) = 0$$

$$\sum_{j=1}^{N} jz^{j-1}[U_{1j}^{(0)}(x, y, -h) + U_{1j}^{(1)}(x, y, -h)] + W_{,x}^{(0)}(x, y, -h) + W_{,x}^{(1)}(x, y, -h) = 0$$

$$\sum_{j=1}^{N} jz^{j-1}[U_{2j}^{(0)}(x, y, -h) + U_{2j}^{(1)}(x, y, -h)] + W_{,y}^{(0)}(x, y, -h) + W_{,y}^{(1)}(x, y, -h) - \frac{1}{R}\sum_{j=0}^{N} z^j[U_{2j}^{(0)}(x, y, -h) + U_{2j}^{(1)}(x, y, -h)] = 0$$

$$\sum_{j=1}^{N} jz^{j-1}[U_{1j}^{(0)}(x, y, z^*) + U_{1j}^{(1)}(x, y, z^*)] + W_{,x}^{(0)}(x, y, z^*) + W_{,x}^{(1)}(x, y, z^*) = 0$$

$$\sum_{j=1}^{N} jz^{j-1}[U_{2j}^{(0)}(x, y, z^*) + U_{2j}^{(1)}(x, y, z^*)] + W_{,y}^{(0)}(x, y, -h) + W_{,y}^{(1)}(x, y, z^*) - \frac{1}{R}\sum_{j=0}^{N} z^j[U_{2j}^{(0)}(x, y, z^*) + U_{2j}^{(1)}(x, y, z^*)] = 0 \quad (7)$$

$$\sum_{j=1}^{N} jz^{j-1}[U_{1j}^{(0)}(x, y, h) + U_{1j}^{(2)}(x, y, h)] + W_{,x}^{(0)}(x, y, h) + W_{,x}^{(2)}(x, y, h) = 0$$

$$\sum_{j=1}^{N} jz^{j-1}[U_{2j}^{(0)}(x, y, h) + U_{2j}^{(2)}(x, y, h)] + W_{,y}^{(0)}(x, y, -h) + W_{,y}^{(2)}(x, y, h) - \frac{1}{R}\sum_{j=0}^{N} z^j[U_{2j}^{(0)}(x, y, h) + U_{2j}^{(2)}(x, y, h) = 0 \quad (x, y) \in \Omega_d$$

$$\sum_{j=1}^{N} jz^{j-1}[U_{1j}^{(0)}(x, y, z^*) + U_{1j}^{(2)}(x, y, z^*)] + W_{,x}^{(0)}(x, y, z^*) + W_{,x}^{(2)}(x, y, z^*) = 0$$

$$\sum_{j=1}^{N} jz^{j-1}[U_{2j}^{(0)}(x, y, z^*) + U_{2j}^{(2)}(x, y, z^*)] + W_{,y}^{(0)}(x, y, -h) + W_{,y}^{(2)}(x, y, z^*) - \frac{1}{R}\sum_{j=0}^{N} z^j[U_{2j}^{(0)}(x, y, z^*) + U_{2j}^{(2)}(x, y, z^*) = 0$$

Using eqns (7), the twelve higher-order terms, denoted, $U_{\alpha N}^{(i)}$, $U_{\alpha(N-1)}^{(i)}$, ($i = 0, 1, 2$; $\alpha = 1,2$), can be identified in terms of the lower-order terms. The detailed expression for these identified higher-order terms with $N = 4$, is presented in the Appendix. It must be noted that an exception arises for mid-surface delamination where $U_{\alpha 1}^{(i)}$ ($i = 1, 2$) should be identified instead of $U_{\alpha(N-1)}^{(i)}$.

Consider a cylindrical shell that is subject to an in-plane compressive load distribution, p, at the mid-surface along the x direction, which is normal to the boundary of the shell (Fig. 1). The principle of the stationary value of the total potential is used to derive the governing equations. For linear buckling analysis, the prebuckling state is assumed to be a membrane primary state since the axial compressive load is applied statically. This is characterized by:

$$\sigma_i = \begin{cases} p & i = 1 \\ 0 & i = 2,4,5,6 \end{cases} \quad (8)$$

The second-order work done by the prebuckling stress can be expressed as follows:

$$\delta W = \int_\Omega phu_{3,x}\delta u_{3,x}\, d\Gamma \quad (9)$$

where W is the work done by the applied compressive loads and Ω is the region of the whole shell. The principle of the stationary value of the total potential is given by:

$$\delta\Pi = \int_\Omega \int_{-h/2}^{h/2} \sigma_i \delta\varepsilon_i\, dz\, d\Omega - \int_\Omega phu_{3,x}\delta u_{3,x}\, d\Gamma = 0 \quad (10)$$

where Π is the total potential energy of the delaminated shell. Following eqns (1)–(4), the strains and stresses can also be written in the following form:

$$\varepsilon_i = \varepsilon_i^{(0)} + [1 - H(z^*)]\varepsilon_i^{(1)} + H(z^*)\varepsilon_i^{(2)} \quad i = 1, 2, \ldots 6 \quad (11)$$

$$\sigma_i = \sigma_i^{(0)} + [1 - H(z^*)]\sigma_i^{(1)} + H(z^*)\sigma_i^{(2)}$$

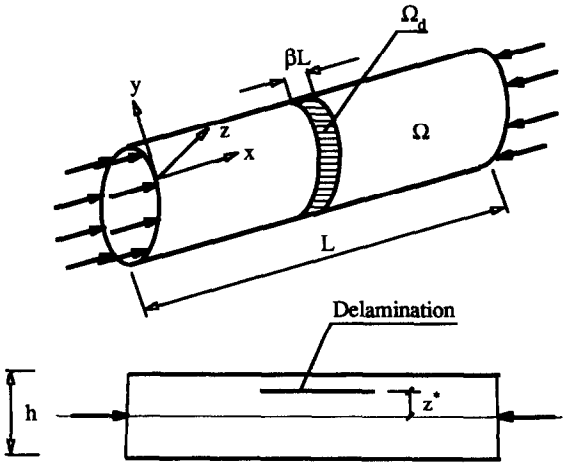

Fig. 1. Geometry of cylindrical shell with delamination.

Equation (9) can now be rewritten based on two integral regions, the non-delamination region $\Omega - \Omega_d$ and the delamination region Ω_d as follows:

$$\int_{\Omega-\Omega_d}\left[\int_{-h/2}^{h/2}\sigma_i^{(0)}\delta\varepsilon_i^{(0)}\,dz - phW_{,x}^{(0)}\delta W_{,x}^{(0)}\right]d\Omega + \int_{\Omega_d}\left\{\int_{-h/2}^{z^*}[(\sigma_i^{(1)}+\sigma_i^{(0)})\delta\varepsilon_i^{(1)}+\sigma_i^{(1)}\delta\varepsilon_i^{(0)}]\,dz - p\left(\frac{h}{2}+z^*\right)[(W_{,x}^{(1)}+W_{,x}^{(0)})\delta W_{,x}^{(1)}+W_{,x}^{(1)}\delta W_{,x}^{(0)}]\right\} + \int_{\Omega_d}\left\{\int_{z^*}^{h/2}[(\sigma_i^{(2)}+\sigma_i^{(0)})\delta\varepsilon_i^{(2)}+\sigma_i^{(2)}\delta\varepsilon_i^{(0)}]\,dz - p\left(\frac{h}{2}-z^*\right)[(W_{,x}^{(2)}+W_{,x}^{(0)})\delta W_{,x}^{(2)}+W_{,x}^{(2)}\delta W_{,x}^{(0)}]\right\}d\Omega = 0 \quad (12)$$

Integration of eqn (11), through the thickness, yields the following equation:

$$\begin{aligned}&\int_{\Omega-\Omega_d}(N_{1j}^{(0)}\delta U_{1j,x}^{(0)}+N_{2j}^{(0)}\delta U_{2j,y}^{(0)}+N_{6j}^{(0)}\delta(U_{1j,y}^{(0)}\\&+U_{2j,x}^{(0)})+N_{5j}^{(0)}\delta[(j+1)U_{1(j+1)}^{(0)}+W_{,x}^{(0)}]\\&+N_{4j}^{(0)}\delta\left[(j+1)U_{2(j+1)}^{(0)}+W_{,y}^{(0)}-\frac{U_{2j}^{(0)}}{R}\right]\\&-phW_{,x}^{(0)}\delta W_{,x}^{(0)}]\,d\Omega\\&+\int_{\Omega_d}\{(N_{1j}^{(1)}+N_{1j}^{(10)})\delta U_{1j,x}^{(1)}\\&+N_{1j}^{(1)}\delta U_{1j,x}^{(0)}+(N_{2j}^{(1)}+N_{2j}^{(10)})\delta U_{2j,y}^{(0)}+N_{2j}^{(1)}\delta U_{2j,y}^{(0)}\\&+(N_{6j}^{(1)}+N_{6j}^{(10)})\delta(U_{1j,y}^{(1)}+U_{2j,x}^{(1)})\\&+N_{6j}^{(1)}\delta(U_{1j,y}^{(0)}+U_{2j,x}^{(0)})\\&+(N_{5j}^{(1)}+N_{5j}^{(10)})\delta[(j+1)U_{1(j+1)}^{(1)}+W_{,x}^{(1)}]\\&+N_{5j}^{(1)}\delta[(j+1)U_{1(j+1)}^{(0)}+W_{,x}^{(0)}]\\&+(N_{4j}^{(1)}+N_{4j}^{(10)})\delta\left[(j+1)U_{2(j+1)}^{(1)}+W_{,y}^{(1)}-\frac{U_{2j}^{(1)}}{R}\right]\\&+N_{4j}^{(10)}\delta\left[(j+1)U_{2(j+1)}^{(0)}+W_{,y}^{(0)}-\frac{U_{2j}^{(0)}}{R}\right]\\&-p\left(\frac{h}{2}+z^*\right)[(W_{,x}^{(1)}+W_{,x}^{(0)})\delta W_{,x}^{(1)}+W_{,x}^{(1)}\delta W_{,x}^{(0)}]\\&+(N_{1j}^{(2)}+N_{1j}^{(20)})\delta U_{1j,x}^{(2)}+N_{1j}^{(2)}\delta U_{1j,x}^{(0)}\\&+(N_{2j}^{(2)}+N_{2j}^{(20)})\delta U_{2j,y}^{(0)}+N_{2j}^{(2)}\delta U_{2j,y}^{(0)}\\&+(N_{6j}^{(2)}+N_{6j}^{(20)})\delta(U_{1j,y}^{(2)}+U_{2j,x}^{(2)})\\&+N_{6j}^{(2)}\delta(U_{1j,y}^{(0)}+U_{2j,x}^{(0)})+(N_{5j}^{(2)}\\&+N_{5j}^{(20)})\delta[(j+1)U_{1(j+1)}^{(2)}+W_{,x}^{(2)}]\\&+N_{5j}^{(2)}\delta[(j+1)U_{1(j+1)}^{(0)}+W_{,x}^{(0)}]\\&+(N_{4j}^{(2)}+N_{4j}^{(20)})\delta\left[(j+1)U_{2(j+1)}^{(2)}+W_{,y}^{(2)}-\frac{U_{2j}^{(2)}}{R}\right]\\&+N_{4j}^{(20)}\delta\left[(j+1)U_{2(j+1)}^{(0)}+W_{,y}^{(0)}-\frac{U_{2j}^{(0)}}{R}\right]\\&-p\left(\frac{h}{2}-z^*\right)[(W_{,x}^{(2)}+W_{,x}^{(0)})\delta W_{,x}^{(2)}+W_{,x}^{(2)}\delta W_{,x}^{(0)}]\Big\}\,d\Omega\\&=0\end{aligned} \quad (13)$$

where the stress resultants are defined as follows:

$$\begin{aligned}N_{ij}^{(0)}&=\int_{-h/2}^{h/2}\sigma_i^{(0)}z^{j-1}\,dz\\N_{ij}^{(1)}&=\int_{-h/2}^{z^*}\sigma_i^{(1)}z^{j-1}\,dz\\N_{ij}^{(10)}&=\int_{-h/2}^{z^*}\sigma_i^{(0)}z^{j-1}\,dz\\N_{ij}^{(2)}&=\int_{z^*}^{h/2}\sigma_i^{(2)}z^{j-1}\,dz\\N_{ij}^{(20)}&=\int_{z^*}^{h/2}\sigma_i^{(0)}z^{j-1}\,dz\end{aligned} \quad (14)$$

Using eqns (1)–(4), the stress resultants in eqn (13) can be expressed in terms of the generalized displacements. Furthermore, replacing the higher-order terms $U_{\alpha N}^{(i)}$, $U_{\alpha(N-1)}^{(i)}$ $(i=0,1,2;\alpha=1,2)$ with the expressions which are identified by solving eqn (7), the final form of eqn (13) is written in terms of the generalized displacement variables $U_{\alpha j}^{(i)}$ $(j=0,1,2,\ldots N-2)$ and $W^{(i)}$. By collecting terms involving the variations of functions $U_{\alpha j}^{(i)}$ and $W^{(i)}$ separately, a total of $3(2N-1)$ governing equations are obtained which are not presented here.

SOLUTION METHODOLOGY

The Rayleigh–Ritz method is used to solve the system of equations derived. The unknown variables of generalized displacements can be expressed in the form of a double infinite trigonometric series. In general, the following form, which satisfies the boundary conditions and continuity conditions, is used here:

$$\begin{aligned}U_{1j}^{(0)}&=\bar{U}_{mn}^{(0j)}\cos\frac{ny}{R}\cos\frac{m\pi x}{L}\\U_{2j}^{(0)}&=\tilde{U}_{mn}^{(0j)}\sin\frac{ny}{R}\sin\frac{m\pi x}{L}\\W^{(0)}&=\bar{W}_{mn}^{(0)}\cos\frac{ny}{R}\Phi_m^{(0)}(x)\\U_{1j}^{(k)}&=\bar{U}_{mn}^{(kj)}\cos\frac{ny}{R}\sin\frac{m\pi(x-l)}{\beta L}\\U_{2j}^{(k)}&=\tilde{U}_{mn}^{(kj)}\sin\frac{ny}{R}\sin\frac{m\pi(x-l)}{\beta L}\qquad k=1,2\\W^{(k)}&=\bar{W}_{mn}^{(k)}\cos\frac{ny}{R}\left[\frac{1}{m}\sin\frac{m\pi(x-l)}{\beta L}\right.\\&\quad\left.-\frac{1}{m+2}\sin\frac{(m+2)\pi(x-l)}{\beta L}\right]\end{aligned} \quad (15)$$

with

$$\Phi_m^{(0)} = \begin{cases} \sin\dfrac{m\pi x}{L} & \text{(simply supported)} \\ \dfrac{1}{m}\sin\dfrac{m\pi x}{L} - \dfrac{1}{m+2}\sin\dfrac{(m+2)\pi x}{L} & \text{(clamped)} \end{cases} \tag{16}$$

where $\bar{U}_{mn}^{(kj)}$, $\tilde{U}_{mn}^{(kj)}$ and $\bar{W}_{mn}^{(k)}$ are unknown coefficients, l represents the delamination position measured from the left end of the shell, β is the delamination length parameter and βL is defined as the dimensional delamination length. Using these solution forms in the governing equation results in $3M(2N-1)$ sets of homogeneous linear algebraic equations in $\bar{U}_{mn}^{(kj)}$, $\tilde{U}_{mn}^{(kj)}$ and $\bar{W}_{mn}^{(k)}$, where $k = 0, 1, 2$; $j = 0, 1, 2, \ldots, N-2$ and $m = 1, \ldots, M$ (only one n due to the orthogonality of $\sin(ny/R)$ and $\cos(ny/R)$). For a non-trivial solution to exist, the determinant of the matrix formed by the coefficients of the above system must be zero. In matrix form, the governing equation is expressed as follows:

$$(\mathbf{K}_L + \lambda \mathbf{K}_G)\mathbf{a} = 0 \tag{17}$$

where $\mathbf{K}_L$ is the linearized direct stiffness matrix, $\mathbf{K}_G$ is the geometric stiffness matrix and λ is the eigenvalue of the system. This eigenvalue problem associated with bifurcation (buckling) analysis is solved to obtain the critical load of the composite cylindrical shell with delamination.

RESULTS AND DISCUSSION

At first, an example of an isotropic cylindrical shell with clamped ends (see Fig. 1) subject to the axial compression is presented to compare the results obtained using the proposed theory with those obtained using classical laminate theory.[7] The delamination lies at $0{\cdot}3h$ from the outer surface (the corresponding thickness parameter of delamination layer, α, defined as $\alpha = 2z^*/h$, is equal to 0·4 in this example) and spans the entire circumference (Fig. 1). The dimensions of the shell are such that $L/R = 5$, and $R/h = 30$, where L is the axial length of the shell. The numerical results of variation of critical load with delamination length, obtained using the present theory, are compared with existing solutions, shown in Fig. 2. In the figure, the circled data points indicate the solutions presented in Ref. 7, in which the transverse shear effects were not included. It is shown that the critical load computed from the classical laminate theory deviates substantially from those derived using the proposed theory. Even when the radius-to-thickness ratio is considerably large ($R/h = 30$) and the material is isotropic, a case for which the classical laminate theory is generally regarded to be accurate for plate, a deviation of about 7·5% is observed in the value of the shell critical buckling load. This indicates that the transverse shear effect plays a very significant role in cylindrical shells. The effects are even larger than those observed in composite plates.[27] This observation agrees with that reported elsewhere,[13] which is for isotropic cylindrical shells the refined theory, and predicts a much lower critical load than the simplified Donnell shell theory. The first-order shear deformation theory shows good agreement with the present theory in this case of isotropic materials.

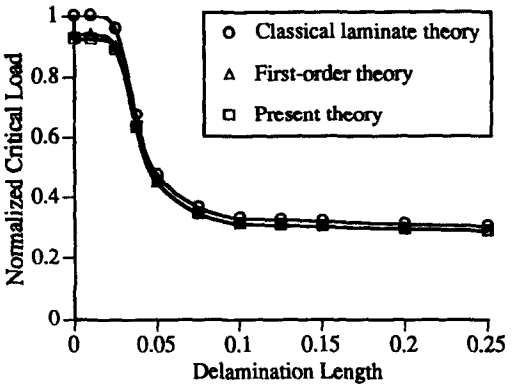

Fig. 2. Effect of transverse shear on critical load for isotropic shell.

With composite materials, the significant effect of transverse shear deformation can be demonstrated more clearly. Therefore, the analysis is performed with shells made of frequently used composites. In this example, composite shells, with the same geometric dimensions as in the first example, are subjected to a uniform in-plane axial compressive load. The stacking sequences of laminates are $[0°/90°/0°]_{10}$ and $[-45°/45°]_{8S}$. Both ends are assumed to be clamped. The materials used are graphite/epoxy and Kevlar/epoxy. The engineering constants, typical of these materials, are presented in Table 1.

The normalized critical load distribution of the $[0°/90°/0°]_{10}$ graphite/epoxy shell is plotted over a range of the radius-to-thickness ratio, R/h, in Fig. 3 for two different values of the non-dimensional delamination length: case (a) $\beta = 0{\cdot}02$, and case (b) $\beta = 0{\cdot}0375$. The figures show significant deviations between solutions obtained using the classical theory and those obtained using the proposed theory. The deviation is more prominent at smaller values of R/h. It is obvious that the transverse shear effects are larger in case (b) than in case (a) due to the changes in local radius-to-thickness ratio. This phenomenon was previously observed[27] when analyzing composite plates with delaminations. As seen from Fig. 3, good agreement is observed between the first-order theory and present theory for the large value of R/h; however, deviations occur for smaller values of R/h. For example, deviations of about 9% in case (a) and about 13% in case (b) are observed from the first-order theory to the present theory. The

Table 1. Material properties

	E_L/E_T	G_{LT}/E_T	G_{TT}/G_{LT}	ν_{LT}
Graphite/epoxy	40	0·5	1·0	0·25
Kevlar/epoxy	15·6	0·56	1·0	0·35

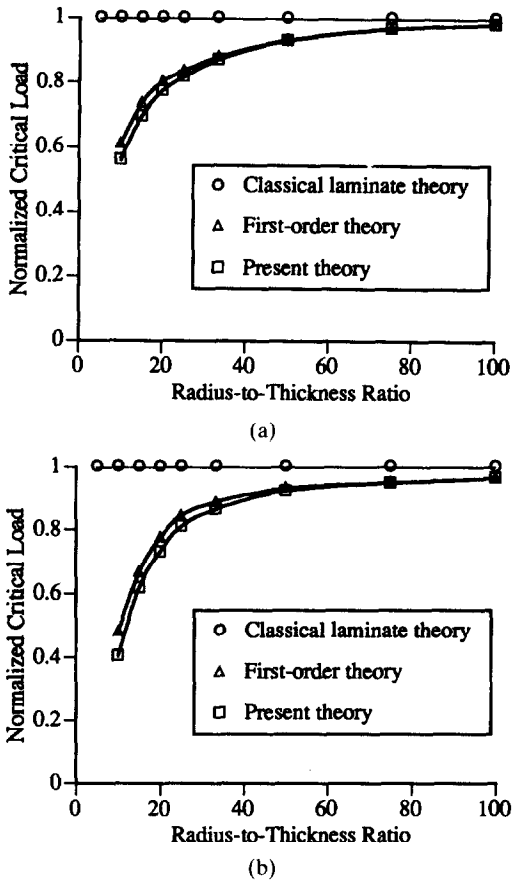

Fig. 3. Effect of transverse shear with variations of radius-to-thickness ratio, graphite/epoxy, $[0°/90°/0°]_{10}$, $\alpha = 0·4$: (a) non-dimensional delamination length, $\beta = 0·0375$; (b) non-dimensional delamination length, $\beta = 0·02$.

normalized critical load distribution of $[-45°/45°]_{8S}$ graphite/epoxy shells is plotted in Fig. 4 and shows larger deviations between the first-order theory and the present theory than those observed for the $[0°/90°/0°]_{10}$ shell. For example, the critical load predicted by the present theory is about 15% lower, for the value of $R/h = 10$, than that predicted by the first-order theory.

Some parametric studies are performed to investigate the effect of material properties. Figure 5 shows a comparison of the present theory with the classical laminate theory for the two different materials, graphite/epoxy and Kevlar/epoxy. As seen from Fig. 5, the larger deviation of results, from the classical laminate theory, occur for graphite/epoxy with higher tensile-to-transverse modules ratio (E_L/E_T) and

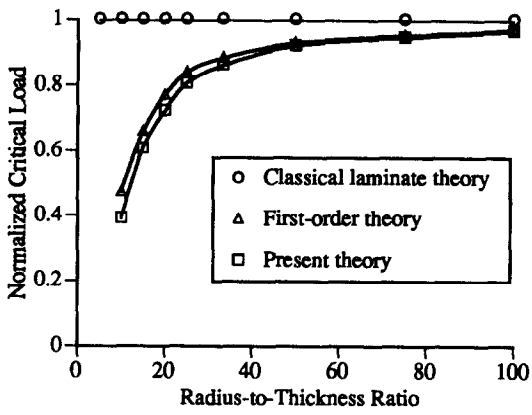

Fig. 4. Effect of transverse shear with variations of radius-to-thickness ratio, graphite/epoxy, $[-45°/45°]_{8S}$, $\alpha = 0·4$, $\beta = 0·02$.

higher transverse-to-shear modulus ratio (E_T/G_{LT}), which is expected. Since these two ratios are generally large for most composite materials, it appears that the transverse shear effect becomes a very significant factor in assessing the delamination buckling behavior of laminates.

Comparisons of the transverse shear effect on the normalized critical load, with changes in the magnitude of the delamination length parameter, β, are presented in Fig. 6 for the $[0°/90°/0°]_{10}$ shell and in Fig. 7 for the $[-45°/45°]_{8S}$ shell. In both cases, the delamination is positioned symmetrically in the axial direction. The figures indicate that in both cases the transverse shear effect becomes smaller as the

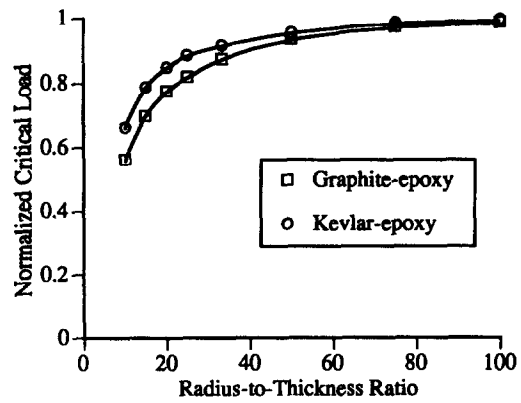

Fig. 5. Comparison of transverse shear effect with variations in material properties, $[0°/90°/0°]_{10}$, $\beta = 0·02$, $\alpha = 0·4$.

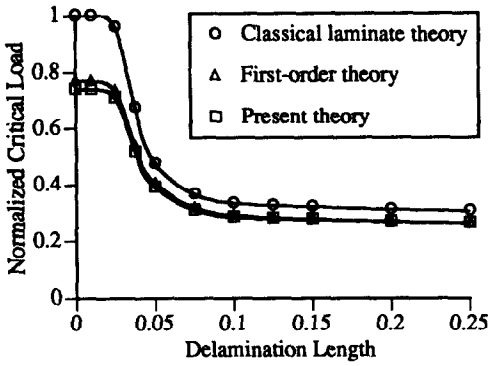

Fig. 6. Effect of transverse shear on critical load, graphite/epoxy, $[0°/90°/0°]_{10}$, $R/h = 20$, $\alpha = 0{\cdot}4$.

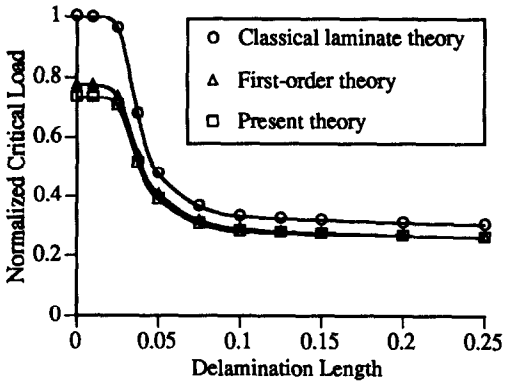

Fig. 7. Effect of transverse shear on critical load, graphite/epoxy, $[-45°/45°]_{8S}$, $R/h = 20$, $\alpha = 0{\cdot}4$.

delamination length increases. This is due to the fact that with the increase in delamination length, local buckling of the delaminated layer becomes dominant which causes the local radius-to-thickness ratio to be larger, and therefore the transverse shear effect decreases. The effect of transverse shear is more dominant in the angle-ply case (Fig. 7) than in the cross-ply case (Fig. 6). Also, slightly larger deviations between the first-order theory and the present theory are observed in the $[-45°/45°]_{8S}$ case, within the whole range of R/h values, as shown in Fig. 7. In general, larger deviations between the first-order theory and the present theory are observed in the composite shells than in the isotropic shells.

Axial distributions of the non-dimensional buckling deflection, $\bar{W}$, and their variations with delamination lengths are plotted in Fig. 8 for the $[0°/90°/0°]_{10}$ graphite/epoxy shell. It is seen from Fig. 8(a) that for short delamination lengths only global buckling occurs and no separation can be observed. When the delamination length reaches an intermediate value, buckling begins with a mixed mode (combined local and global), as shown in Fig. 8(b). The deflection modes for the delaminated layer and the entire laminate are now coupled as observed from this figure. For a longer delamination length local buckling is dominant, and, as shown in Fig. 8(c), only the buckling of the delaminated layer is observed. This stage can be refered to as the transition stage where transition from global to local buckling occurs.

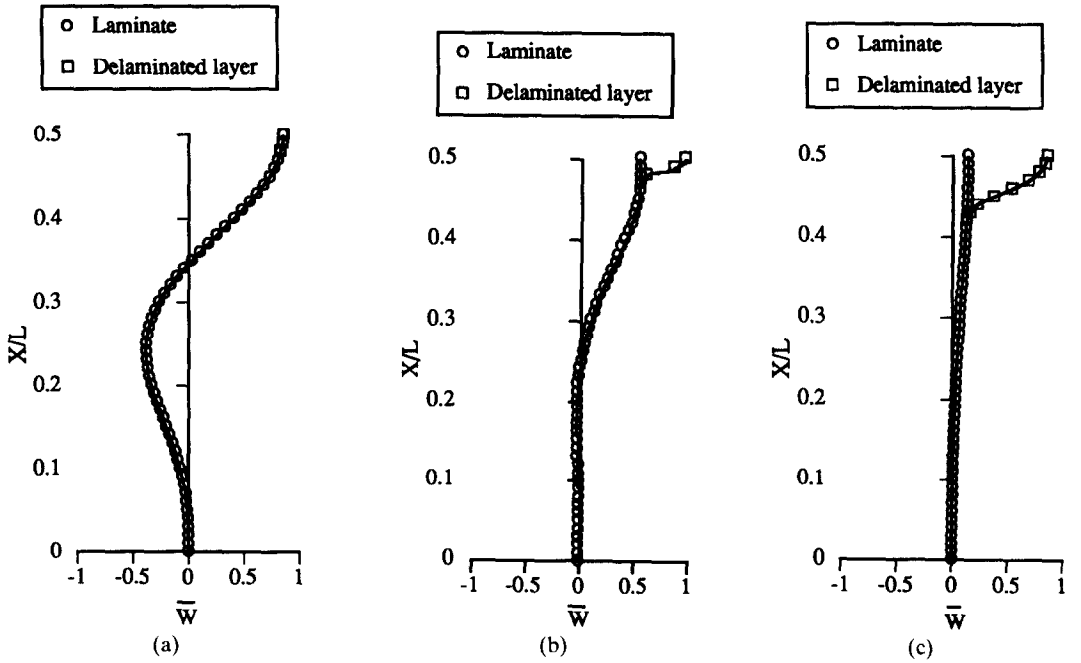

Fig. 8. Buckling mode for deflection of shells with various delamination lengths, graphite/epoxy, $[0°/90°/0°]_{10}$, $R/h = 20$, $\alpha = 0{\cdot}4$: (a) $\beta = 0{\cdot}025$; (b) $\beta = 0{\cdot}04$; (c) $\beta = 0{\cdot}15$.

CONCLUDING REMARKS

A new higher-order theory has been developed to study the delamination buckling problem in composite cylindrical shells. The refined displacement field proposed in this paper is capable of representing displacement discontinuity conditions at the interface of the existing delamination as well as in satisfying the transverse shear stress-free conditions at surfaces and at the delamination interface. Numerical investigations of the transverse shear effect on buckling load were performed. Comparisons were made with the classical theory and a first-order theory. The following important observations were made:

(1) The present theory provides an adequate framework for the analysis of composite cylindrical shells with delaminations. Particularly, the theory is expected to give accurate displacement distributions with lower computational cost for engineering applications.
(2) For laminated composite shells, the transverse shear effect on delamination buckling is very significant. The effect is more pronounced in case of angle-ply laminates and in materials with a higher value of tensile-to-shear modulus.
(3) Larger deviations are observed between the present theory and the classical theory even for thin isotropic shells. Significant deviations observed between the present theory and the first-order theory for thick composite shells indicate the importance of the transverse shear effects.
(4) The transverse shear effect is larger in cases with smaller delamination. This is due to the fact that the mixed buckling mode is more dominant in such cases.

ACKNOWLEDGEMENT

The research was supported by the US Army Research Office under grant number DAAH04-93-G-0043. Technical monitor: Dr Gary Anderson.

REFERENCES

1. Chai, H. & Babcock, C. D., Two-dimensional modeling of failure in laminated plates by delamination buckling. *J. Comp. Mater.*, **19** (1985) 67–98.
2. Sallam, S. & Simitses, G. J., Delamination buckling and growth of flat, cross-ply laminates. *J. Comp. Struct.*, **4** (1985) 361–81.
3. Barbero, E. J. & Reddy, J. N., Modeling of delamination in composite laminates using a layer-wise plate theory. *Int. J. Solid Struct.*, **28** (1991) 373–88.
4. Jones, R. M., Buckling of stiffened two-layered shell of revolution with a circumferentially cracked unbonded layer. *AIAA J.*, **7**, (1969) 1511–17.
5. Kulkarni, S. V. & Frederick, D., Buckling of partially debonded layered cylindrical shell. *Proc. AIAA/ASME/SAE 14th SDM Conf.*, Williamsburg, VA, 1973.
6. Troshin, V. P., Effect of longitudinal delamination in a laminar cylindrical shell on the critical external pressure. *J. Comp. Mater.*, **17** (1983) 563–7.
7. Sallam, S. & Simitses, G. J., Delamination buckling of cylindrical shells under axial compression. *J. Comp. Struct.*, **7** (1987) 83–101.
8. Simitses, G. J. & Chen, Z. Q., Buckling of delaminated long cylindrical panels under pressure. *Computers and Structures*, **28** (1988) 173–84.
9. Chen, Z. Q. & Simitses, G. J., Delamination buckling of pressure-loaded, cross-ply laminated cylindrical shells. *ZAMM Z. angew. Math. Mech.*, **68** (1988) 491–501.
10. Chang, F. K. & Kutlu, Z., Delamination effects on composite shells. *J. Eng. Mater.*, **112** (1990) 336–40.
11. Kardomateas, G. A. & Chung, C. B., Thin film modeling of delamination buckling in pressure loaded laminated cylindrical shells. *AIAA J.*, **30** (1992) 2119–23.
12. Bhaskar, K. & Varadan, T. K., Exact elasticity solution for laminated anisotropic cylindrical shells. *J. Appl. Mech.*, **60** (1993) 41–7.
13. Kardomateas, G. A., Stability loss in thick transversely isotropic cylindrical shells under axial compression. *J. Appl. Mech.*, **60** (1993) 506–13.
14. Reddy, J. N. & Savoia, M., Layer-wise shell theory for postbuckling of laminated circular cylindrical shells. *AIAA J.*, **30** (1992) 2148–54.
15. Reddy, J. N. & Liu, C. F., A higher-order shear deformation theory of laminated elastic shells. *Int. J. Eng. Sci.*, **23** (1985) 319–30.
16. Stein, M., Nonlinear theory for plate and shells including the effects of transverse shearing. *AIAA J.*, **24** (1986) 1537–44.
17. Lu, V. P. & Chia, C. Y., Effect of transverse shear on nonlinear vibration and postbuckling of antisymmetric cross-ply imperfect cylindrical shells. *Int. J. Solids Struct.*, **29** (1988) 195–210.
18. Denis, S. T. & Palazotto, A. N., Transverse shear deformation in orthotropic cylindrical pressure vessels using a higher-order shear theory. *AIAA J.*, **27** (1989), 1441–7.
19. Khdeir, A. A., Librescu, L. & Frederick, D., A shear deformable theory of laminated composite shallow shell-type panels and their response analysis. *Acta Mechanica*, **76** (1989) 1–13; **77** (1989) 1–20.
20. Donnell, L. H., Thick general shells under general loading. *J. Appl. Mech.* **56** (1989) 391–4.
21. Elishakoff, I., Cederbaum, G. & Librescu, L., Response of moderately thick laminated cross-ply composite shells subjected to random excitation. *AIAA. J.*, **27** (1989) 975–81.
22. Barbero, E. J., Reddy, J. N. & Tepley, J. L., General two-dimensional theory of laminated cylindrical shells. *AIAA. J.*, **28** (1990) 544–53.
23. Simitses, G. J. & Anastasiadis, J. S., Shear deformable theories for cylindrical laminates—equilibrium and buckling with applications. *AIAA J.*, **30** (1992) 826–34.
24. Rychter, Z., A family of shear deformation theories for shallow shells. *Acta Mechanica*, **98** (1993) 221–32.
25. He, L. H., A linear theory of laminated shells accounting for continuity of displacements and transverse shear stresses at layer interfaces. *Int. J. Solids Struct.*, **31** (1994) 613–27.
26. McCarthy, R. E., Three dimensional nonlinear dynamic finite element analysis for the response of a thick

laminated shell to impact loads. AIAA Paper 85-0584, New York, April 1985.
27. Chattopadhyay, A. & Gu, H., A new higher-order plate theory in modeling delamination buckling of composite laminates. *AIAA J.*, **32** (1994) 1709–16.
28. Lo, K. H., Christensen, R. M. & Wu, E. M., A higher-order theory of plate deformation, Part 2: Laminate plates. *J. Appl. Mech.*, **44** (1977) 669–76.

APPENDIX: IDENTIFICATION OF HIGHER-ORDER TERMS

The expressions of identified higher-order terms solved in eqn (7) are given here for the special case of $N = 4$.

$$U_{13}^{(0)} = -\frac{4}{3h^2}(U_{11}^{(0)} + W_{,x}^{(0)})$$

$$U_{14}^{(0)} = -\frac{2}{h^2}U_{12}^{(0)}$$

$$U_{23}^{(0)} = -\frac{64R(RW_{,y}^{(0)} - U_{20}^{(0)}) + 4(16R^2 - h^2)U_{21}^{(0)} - 8Rh^2U_{22}^{(0)}}{(48R^2 - h^2)h^2}$$

$$U_{24}^{(0)} = -\frac{16(RW_{,y}^{(0)} - U_{20}^{(0)}) - 32RU_{22}^{(0)} + 4(24R^2 - h^2)U_{22}^{(0)}}{(48R^2 - h^2)h^2}$$

$$\begin{aligned}U_{13}^{(1)} = &-\frac{4}{3h^2\alpha^2}[(1-\alpha)(U_{11}^{(1)} + W_{,x}^{(0)}) \\ &+ h\alpha(1-\alpha)(U_{12}^{(1)} + U_{12}^{(0)}) \\ &+ (1-\alpha+\alpha^2)(U_{11}^{(1)} + W_{,x}^{(1)})]\end{aligned}$$

$$U_{14}^{(1)} = -\frac{2(1-\alpha)}{h^3\alpha^2}\left[U_{11}^{(1)} + W_{,x}^{(0)} + h\alpha\left(\frac{U_{12}^{(1)}}{1-\alpha} + U_{12}^{(0)}\right) + U_{11}^{(1)} + W_{,x}^{(1)}\right]$$

$$\begin{aligned}U_{23}^{(1)} = &-\frac{2}{h^2\alpha^2[(8R+h)(6R-h\alpha) + \alpha(8R-h\alpha)(6R+h)]} \\ &\times\{2(8R+h)(2R-h\alpha) \\ &+ \alpha^3(8R-h\alpha)(2R+h)]U_{21}^{(1)} \\ &+ h\alpha[(8R+h)(4R-h\alpha) \\ &- \alpha^2(8R-h\alpha)(4R+h)]U_{22}^{(1)} \\ &+ 4[8R + h + \alpha^3(8R-h\alpha)](RW_{,y}^{(1)} - U_{20}^{(1)}) \\ &+ 2(8R+h)\left[2R - h\alpha - \alpha^2 \times\frac{(16R^2-h^2)(6R-h\alpha) - 4Rh\alpha(8R-h\alpha)}{(48R^2-h^2)}\right]U_{21}^{(0)} \\ &+ h\alpha(8R+h)\left[4R - h\alpha + \alpha \times\frac{4Rh(6R-h\alpha) - \alpha^2(24R^2-h^2)(8R-h\alpha)}{(48R^2-h^2)}\right]U_{22}^{(0)} \\ &+ 4(8R+h)\left[1 - \alpha^2\frac{8R(6R-h\alpha) + h\alpha(8R-h\alpha)}{(48R^2-h^2)}\right] \times(RW_{,y}^{(0)} - U_{20}^{(0)})\Big]\end{aligned}$$

$$\begin{aligned}U_{24}^{(1)} = &-\frac{4}{h^3\alpha^2[(8R+h)(6R-h\alpha) + \alpha(8R-h\alpha)(6R+h)]} \\ &\times\{2[(6R+h)(2R-h\alpha) \\ &- \alpha^2(6R-h\alpha)(2R+h)]U_{21}^{(1)} \\ &+ h\alpha[(6R+h)(4R-h\alpha) \\ &+ \alpha(6R-h\alpha)(4R+h)]U_{22}^{(1)} \\ &+ 4[6R + h - \alpha^2(6R-h\alpha)](RW_{,y}^{(1)} - U_{20}^{(1)}) \\ &+ 2(6R+h)\left[2R - h\alpha - \alpha^2 \times\frac{(16R^2-h^2)(6R-h\alpha) - 4Rh\alpha(8R-h\alpha)}{(48R^2-h^2)}\right]U_{21}^{(0)} \\ &+ h\alpha(6R+h)\left[4R - h\alpha + \alpha \times\frac{4Rh(6R-h\alpha) - \alpha(24R^2-h^2)(8R-h\alpha)}{(48R^2-h^2)}\right]U_{22}^{(0)} \\ &+ 4(6R+h)\left[1 - 4\alpha^2 \times\frac{8R(6R-h\alpha) - h\alpha(8R-h\alpha)}{(48R^2-h^2)}\right](RW_{,y}^{(0)} - U_{20}^{(0)})\Big\}\end{aligned}$$

$$\begin{aligned}U_{13}^{(2)} = &-\frac{4}{3h^2\alpha^2}[(1+\alpha)(U_{11}^{(2)} + W_{,x}^{(0)}) \\ &+ h\alpha(1+\alpha)(U_{12}^{(2)} + U_{12}^{(0)}) \\ &+ (1+\alpha+\alpha^2)(U_{11}^{(2)} + W_{,x}^{(2)})]\end{aligned}$$

$$U_{14}^{(2)} = \frac{2(1+\alpha)}{h^3\alpha^2}\left[U_{11}^{(2)} + W_{,x}^{(2)} + h\alpha\left(\frac{U_{12}^{(2)}}{1+\alpha} + U_{12}^{(0)}\right) + U_{11}^{(2)} + W_{,x}^{(2)}\right]$$

$$\begin{aligned}U_{23}^{(2)} = &-\frac{2}{h^2\alpha^2[(8R+h)(6R-h\alpha) - \alpha(8R-h\alpha)(6R+h)]} \\ &\times\Big\{2[(8R+h)(2R-h\alpha) \\ &- \alpha^3(8R-h\alpha)(2R+h)]U_{21}^{(2)} \\ &+ h\alpha[(8R+h)(4R-h\alpha) \\ &- \alpha^2(8R-h\alpha)(4R+h)]U_{22}^{(2)} \\ &+ 4[8R + h - \alpha^3(8R-h\alpha)](RW_{,y}^{(2)} - U_{20}^{(2)}) \\ &+ 2(8R+h)\Big[2R - h\alpha - \alpha^2\end{aligned}$$

$$\times\frac{(16R^2-h^2)(6R-h\alpha)-4Rh\alpha(8R-h\alpha)}{(48R^2-h^2)}\Big]U_{21}^{(0)}$$

$$+h\alpha(8R+h)\Big[4R-h\alpha-\alpha$$

$$\times\frac{4Rh(6R-h\alpha)-\alpha^2(24R^2-h^2)(8R-h\alpha)}{(48R^2-h^2)}\Big]U_{22}^{(0)}$$

$$+4(8R+h)\Big[1-\alpha^2\frac{8R(6R-h\alpha)+h\alpha(8R-h\alpha)}{(48R^2-h^2)}\Big]$$

$$\times(RW_{,y}^{(0)}-U_{20}^{(0)})\Big\}$$

$$U_{24}^{(2)}=$$

$$-\frac{4}{h^3\alpha^2[(8R+h)(6R-h\alpha)-\alpha(8R-h\alpha)(6R+h)]}$$

$$\times\Big\{2[(6R+h)(2R-h\alpha)$$

$$-\alpha^2(6R-h\alpha)(2R+h)]U_{21}^{(2)}$$

$$+h\alpha[(6R+h)(4R-h\alpha)$$

$$-\alpha(6R-h\alpha)(4R+h)]U_{22}^{(2)}$$

$$+4[6R+h-\alpha^2(6R-h\alpha)](RW_{,y}^{(2)}-U_{20}^{(2)})$$

$$+2(6R+h)\Big[2R-h\alpha-\alpha^2$$

$$\times\frac{(16R^2-h^2)(6R-h\alpha)-4Rh\alpha(8R-h\alpha)}{(48R^2-h^2)}\Big]U_{21}^{(0)}$$

$$+h\alpha(6R+h)\Big[4R-h\alpha+\alpha$$

$$\times\frac{4Rh(6R-h\alpha)-\alpha^2(24R^2-h^2)(8R-h\alpha)}{(48R^2-h^2)}\Big]U_{22}^{(0)}$$

$$+4(6R+h)\Big[1-4\alpha^2$$

$$\times\frac{8R(6R-h\alpha)+h\alpha(8R-h\alpha)}{(48R^2-h^2)}\Big](RW_{,y}^{(0)}-U_{20}^{(0)})\Big\}$$

with

$$\alpha=2z^*/h$$